

# Advanced Flattening Method for Scanned Atomic Force Microscopy Images

Cheolsu HAN

*Department of Electrical and Computer Engineering, Hanyang University, Seoul 133-791, Korea*

Chung Choo CHUNG\*

*Division of Electrical and Biomedical Engineering, Hanyang University, Seoul 133-791, Korea*

(Received 12 December 2011, in final form 20 January 2012)

This paper presents an advanced flattening method to precisely analyze nanostructures by using atomic force microscopy. Distortions caused by the slope of a sample and nonlinearities of the  $Z$  scanner can affect the height of the scanned image and make the scanned image difficult to use for quantitative analysis. We propose an advanced flattening method to flatten an image that does not require the user to be experienced. The distortions can be measured and systematically removed from a scanned image. The proposed method is able to substantially reduce both the artifacts caused by flattening and the inspection time using a scanned image.

PACS numbers: 07.79.Lh

Keywords: Atomic force microscopy, Flattening process, Histogram

DOI: 10.3938/jkps.60.680

## I. INTRODUCTION

A scanned atomic force microscope (AFM) image can be distorted by undesirable factors, such as nonlinearities of the nano-actuator, the slope of the sample, and the tip shape [1–4]. These sources of distortion should be removed for precise analysis because they make the scanned image difficult to analyze quantitatively. The sources of distortion can be classified into four main sources: creep and hysteresis of the piezoelectric actuator, installation slope of a sample, and image bow [4, 5]. These distortions can be measured from a scanned image and can be eliminated [2,6–8].

Many researcher have developed various algorithms for eliminating the distortions, such as the leveling algorithm [5], the coordinate transformation [4,8], the automatic drift elimination method [9], and the vertical and lateral drift correction method [6]. The image bow can be represented by a polynomial [5]. However, the polynomial should be renewed whenever the AFM system is changed. For this reason, a new system was developed with a decoupled scanner system in which the  $Z$  scanner is separated from the  $X$ - $Y$  scanner [10].

Even though reconstruction algorithms have been developed, commercial AFMs provide users with flattening tools that can be implemented by applying  $n^{th}$ -order polynomial fits to each scan line (or plane) [11,12]. Additional artifacts may occur due to the processing direc-

tion of the flattening method. If this problem is to be avoided, skilled users with prior knowledge of the samples are required.

In this paper, under the assumption that the background of the sample is almost flat, we propose an advanced flattening method using a single scanned image. This method applies advantages of both the flattening method using a polynomial fitting curve and the reconstruction method.

## II. EXPERIMENTS AND DISCUSSION

A scanned AFM image was used to verify the proposed method. A calibration sample (TGQ1, NT-MDT, Russia) was employed to obtain a scanned image. The scan range was set to  $20 \times 20 \mu\text{m}^2$ , with an image resolution of  $256 \times 256$  points and a scan rate of 0.5 Hz. The AFM was operated in the constant-force, non-contact mode. The total scanning time for obtaining an image was approximately 9 min. The fast and the slow scanning directions were set to the  $Y$ - and the  $X$ -axes, respectively.

The AFM image shown Fig. 1 was obtained by scanning a sample. Here, the fast scanning direction is along the  $Y$ -axis while the slow scanning direction is along the  $X$ -axis. In this case, the coordinate  $(1, N_y)$  of the scanned image is the starting position, and  $(N_x, N_y)$  is the final position.

The scanned topographic image  $H_t(x, y)$  at  $(x, y)$  may be described by

\*E-mail: cchung@hanyang.ac.kr; Tel: +82-2-2220-1724, Fax: +82-2-2291-5307

$$H_t(x, y) = H_h(x, y) + H_{crp}(x, y) + H_{slp}(x, y), \quad (1)$$

where  $H_h(x, y)$  is the height of the real topography,  $H_{crp}(x, y)$  is the height caused by the creep of the  $Z$  scanner, and  $H_{slp}(x, y)$  is the height caused by the sample tilting at  $(x, y)$ . The tilting angle of the  $Y$ -axis can be determined from the slope of the scanned image along the fast scanning axis. The tilt plane,  $H_{slpY}(x, y)$ , between the sample surface and the fast scanning plane may be parameterized with the 1<sup>st</sup>-order polynomial  $c_y y$ , where  $c_y$  is the slope coefficient in the fast scanning direction.

However, because the proposed method uses a single scanned image, we cannot measure the tilting angle of the sample in the slow scanning  $X$ -axis. We can obtain an image  $H_{crpslpX}(x, y)$  by removing the tilt image  $H_{slpY}(x, y)$  for the fast scanning axis from the scanned image. This image (*i.e.*, heights along the  $Z$ -axis) contains important information including the topographic height of the sample, the creep and hysteresis effects of the  $Z$  scanner, and the slope of the sample in the slow scanning axis. For the measurement of the creep effect of the  $Z$  scanner and the slope effect of the sample in the slow scanning  $X$  direction, the scanned image is projected on the  $X$ - $Z$  plane after the tilt image for the  $Y$ -axis has been removed. A baseline of the profile on the  $X$ - $Z$  plane represents the creep effect of the  $Z$  scanner and the slope effect of the sample in the slow scanning  $X$ -axis. We can construct a creep-slope image by using the baseline.

The baseline of the image projected on the  $X$ - $Z$  plane,  $H_{crpslpX}(x, \cdot)$ , may be described by

$$\begin{aligned} H_{crpslpX}(x, \cdot) &\cong H_{crp}(x, \cdot) + H_{slpX}(x, \cdot) \\ &= p_1 x^n + p_2 x^{n-1} + \dots + p_{n+1}, \end{aligned} \quad (2)$$

where  $H_{crp}(x, \cdot)$  is the slope of the scanned image caused by the creep effect of the  $Z$  scanner in the  $X$ -axis. The creep effect occurs slowly in the slow scanning direction [2, 13].  $H_{slpX}(x, \cdot)$  ( $= c_x x$ ) is the slope of scanned image caused by the sample tilt in the  $X$ -axis, and  $c_x$  is the slope coefficient in the  $X$  direction. The parameters  $\{p_1, p_2, \dots, p_n, p_{n+1}\}$  are the coefficients of the polynomial that represents the baseline, and  $n$  is the order of the polynomial and an integer.

The flattened image  $H_{FLT}(x, y)$ , which is obtained by using the advanced flattening method, is represented by the following equation:

$$\begin{aligned} H_{FLT}(x, y) &= (H_t(x, y) - H_{slpY}(x, y)) \\ &\quad - H_{crpslpX}(x, y). \end{aligned} \quad (3)$$

Here, it is assumed that the image data from the hysteresis of the  $Z$  scanner are negligible [2] and that the background of the sample is almost flat.

Figure 1 shows the scanned image of the calibration sample and the histogram. The scanned image is tilted along the  $X$ - and the  $Y$ -axes relative to the origin (1,

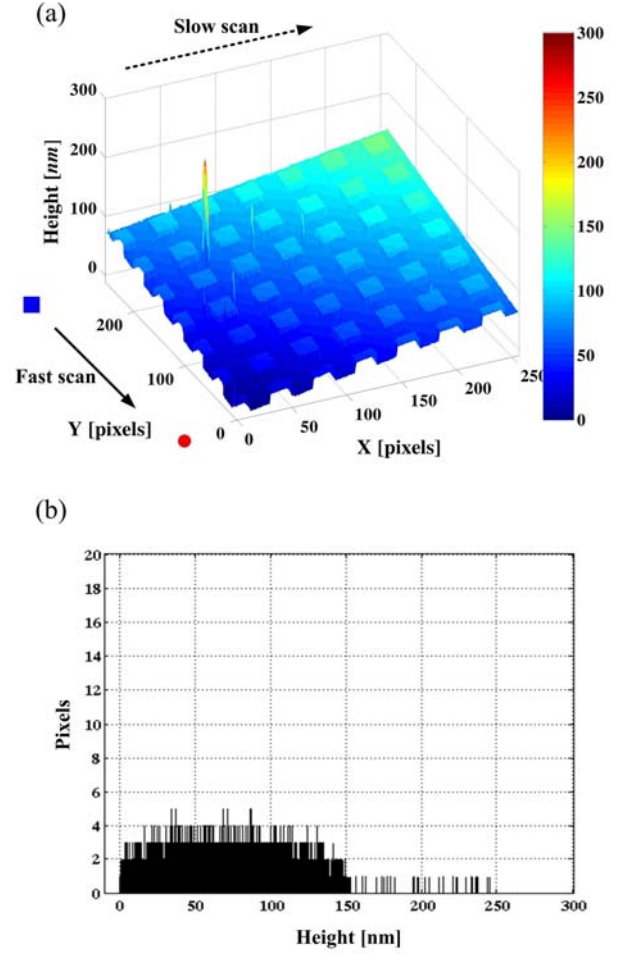


Fig. 1. (Color online) (a) Scanned topographic image and (b) histogram graph.

1) in Fig. 1(a). The histogram shows the height distribution in the image with the number of pixels for each height. The number of pixels is distributed evenly at a particular height in Fig. 1(b). The histogram illustrates the fact that the sample is tilted. The scanned image requires flattening or reconstruction processes to precisely measure the heights or the widths of the nanostructures. The sample is tilted by approximately  $0.2^\circ$  along the  $Y$ -axis relative to the origin (1,1). The slope coefficient,  $c_y$ , is  $3.7 \times 10^{-3}$ . Two levels (0.0 nm and 19.5 nm) exist on the calibration sample. Two peaks should have existed in the histogram graph of the scanned image of the calibration sample in Fig. 1(b).

Figure 2 shows the flattened images that were obtained by applying the flattening method and associated histograms. Even though the same flattening process was applied to the same scanned image, the flattened images were different. The flattened images in Figs. 2(a) and (b) were obtained by processing the flattening line along the  $X$ - and the  $Y$ -axis directions, respectively. This flattening method modifies the image on a line-by-line basis, removing the vertical offset between scan lines in the flat-

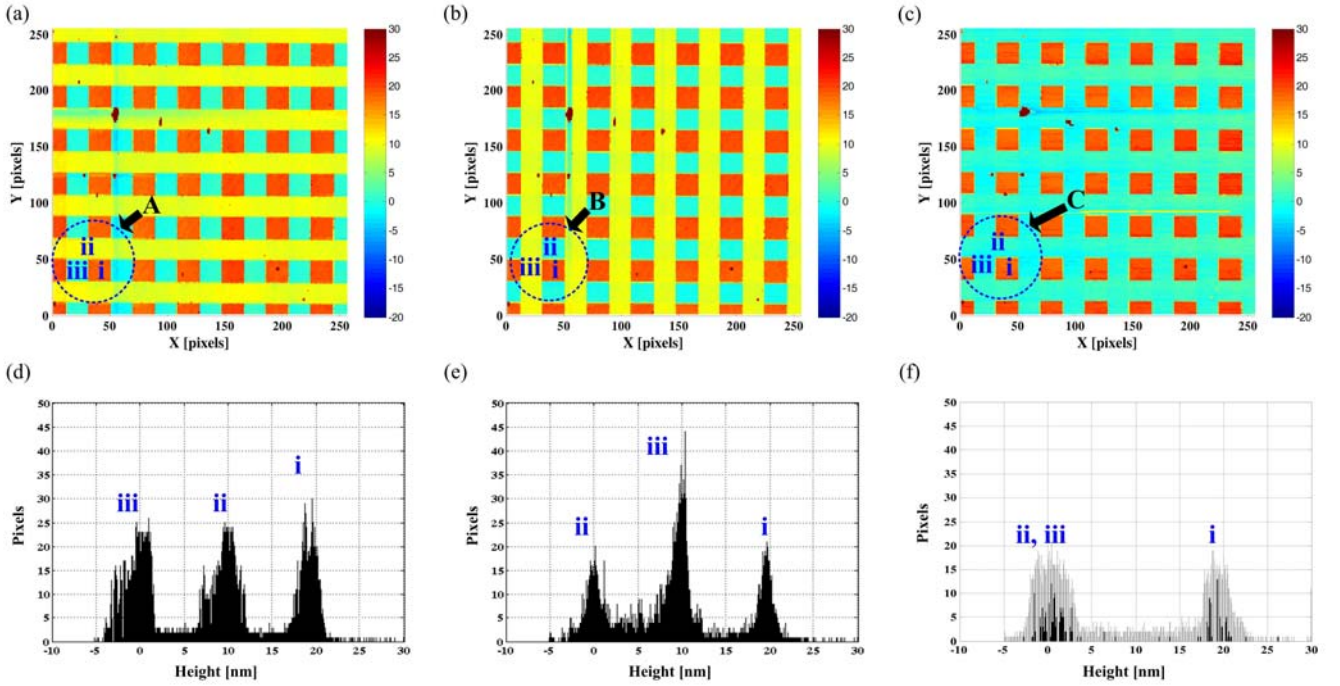


Fig. 2. (Color online) Flattened images generated using the flattening processing tool: (a)  $X$ -axis, (b)  $Y$ -axis, and (c) proposed method. (d), (e) and (f) Histograms for the flattened images in (a), (b) and (c), respectively.

tening process direction by calculating a least-squares-fit polynomial for a scan line and subtracting it from the polynomial fitting line for the original line. This method makes the average  $Z$  value of each scan line equal to zero [11,12]. Even though there are two levels on the calibration sample, three levels were measured on the flattened images. The results of the measurement are summarized in Table 1. Statistics on levels for three different areas (i, ii, and iii) in Figs. 2(a), (b), and (c) are listed. The three peaks were also observed in the histograms of the flattened images (Figs. 2(d) and (e)). Because a flattened image is obtained by calculating the offset between each point on the scan line and the corresponding point on the fitting curve, it can be affected by variations in the scanned data on the line. For this reason, the scanned images appeared different along the processing direction for the flattening process on the line. Commercial AFMs provide special functions, such as inclusion and exclusion, to avoid these problems. However, these functions also require a skilled user to precisely measure the nanostructure [11,12].

Figures 2(c) and (f) show the flattened image and histogram obtained using the proposed method. Three levels exist in the flattened image (resulting measurements are also summarized in Table 1), but two peaks are located close together in the histogram of the flattened image (Fig. 2(f)). The levels of areas ii and iii in Fig. 2(c) were nearly the same. These results were close to the specifications for the calibration sample. The heights are summarized in Table 2.

In commercial AFMs, we commonly use the 2-dimen-

Table 1. Levels of flattened images (units = [nm]).

	area i	area ii	area iii
specification of TGQ1	$19.5 \pm 1.5$	$0.0 \pm 1.5$	$0.0 \pm 1.5$
Fig. 2(a)	$19.6 \pm 1.8$	$9.7 \pm 1.3$	$0.2 \pm 0.7$
Fig. 2(b)	$19.6 \pm 1.7$	$-0.5 \pm 0.4$	$10.0 \pm 0.2$
Fig. 2(c)	$18.8 \pm 0.8$	$0.8 \pm 1.1$	$-0.7 \pm 0.9$

Table 2. Relative heights after flattening (units = [nm]).

	i-ii	i-iii	ii-iii
specification of TGQ1	$19.5 \pm 1.5$	$19.5 \pm 1.5$	$0.0 \pm 1.5$
Fig. 2(a)	$9.9 \pm 2.1$	$19.4 \pm 1.2$	$9.4 \pm 1.2$
Fig. 2(b)	$20.1 \pm 1.8$	$9.6 \pm 1.7$	$10.5 \pm 0.4$
Fig. 2(c)	$17.9 \pm 0.9$	$19.5 \pm 0.7$	$1.5 \pm 1.0$

sional (2D) flattening method to remove tilt or bow from scanned images. The 2D flattening method calculates a single polynomial fit for the entire scanned image and then subtracts the polynomial fit from the scanned image. The 2D flattening method is applied by calculating a 1<sup>st</sup>-, 2<sup>nd</sup>-, 3<sup>rd</sup>-, or 4<sup>th</sup>-order polynomial fit to the image in the  $X$  or the  $Y$  direction. This method also requires a skilled user to precisely reconstruct the real topographic image.

### III. CONCLUSION

An advanced flattening method to precisely analyze nanostructures with AFM is proposed in this paper. Distortions caused by the slope of a sample or nonlinearities of the  $Z$  scanner can affect the height data of the scanned image and make the scanned image difficult to analyze quantitatively. The advanced flattening method we propose does not require extensive user experience. The distortions can be measured and systematically removed from a single scanned image. The proposed method substantially reduces the artifacts caused by the flattening process and the inspection time using a single scanned image. Furthermore, neither directional considerations of the flattening process nor a determination of a numerical new creep model of the  $Z$  scanner are required in our method.

### ACKNOWLEDGMENTS

This work was supported by the International Research & Development Program of the National Research Foundation of Korea (NRF) funded by the Ministry of Education, Science and Technology (MEST) of Korea (grant number K21003001810-11E0100-01510) and the Seoul R&D Program (10919).

### REFERENCES

- [1] E. Ribeiro and M. Shah, *Mach. Vision Appl.* **17**, 147 (2006).
- [2] C. Han and C. Chung, *Rev. Sci. Instrum.* **82**, 053709 (2011).
- [3] F. Marinello, P. Bariani, S. Carmignato and E. Savio, *Meas. Sci. Technol.* **20**, 084013 (2009).
- [4] F. Marinello, S. Carmignato, A. Voltan, E. Savio and L. De Chiffre, *J. Manuf. Sci. Eng.* **132**, 030903 (2010).
- [5] H. Edwards, R. McGlothlin and U. Elisa, *J. Appl. Phys.* **83**, 3952 (1998).
- [6] P. Rahe, R. Bechstein and A. Kuhnle, *J. Vac. Sci. Technol., B* **28**, C4E31 (2010).
- [7] V. Yurov and A. Klimov, *Rev. Sci. Instrum.* **65**, 1551 (1994).
- [8] F. Marinello, P. Bariani, L. De Chiffre and E. Savio, *Meas. Sci. Technol.* **18**, 689 (2007).
- [9] R. Lapshin, *Meas. Sci. Technol.* **18**, 907 (2007).
- [10] J. Kwon, J. Hong, Y. Kim, D. Lee, K. Lee, S. Lee and S. Park, *Rev. Sci. Instrum.* **74**, 4378 (2003).
- [11] Park systems corp., available: <http://www.parkafm.com>.
- [12] Veeco inc., available: <http://www.veeco.com>.
- [13] H. Jung, J. Shim and D. Gwon, *Nanotechnology* **12**, 14 (2001).